

# LOCAL POST-STRENGTHENING OF IN-PLANE LOADED MASONRY WALLS WITH FIBRE-REINFORCED POLYMERS (FRP)

Uwe Pfeiffer, Werner Seim  
Department of Structural Engineering (IKI)  
University of Kassel  
Kassel, Germany

## SUMMARY

This report describes the first investigations for the development of a new analytical model for masonry walls strengthened locally by use of Fibre-Reinforced Polymers (FRPs). The model consists of three steps: first, the description of the load transfer of the strengthened structure; second, the anchorage of the FRP end-region and third, the description of bond characteristics between FRP and masonry unit. Step three of the model was experimentally validated with bonding tests on 33 single masonry units. Step two was experimentally investigated with 24 wall specimens. Six of them will be in this report. Three types of lime-sand bricks and one type of clay brick were used in combination with glass-fibre sheets. Two different types of epoxy resin were used to investigate the effect of adhesives on bond strength.

## INTRODUCTION

A lot of research was carried out over the last decades on post-strengthened masonry walls with a considerable part focussing on shear strength and ductility, in particular for earthquake impacts eg. *Schwegler (1994)*, *ElGawady (2004)* and *Wallner et al. (2005)*. For this purpose Fibre-Reinforced Polymers were applied to the entire wall or like strips. In most cases FRPs were anchored to adjacent reinforced concrete elements like ground beams or floor slabs. However, *Seim et al. (2003)* have already demonstrated that FRPs can also be effectively used for local post-strengthening of in-plane loaded masonry walls. This might be of importance, for example, for additional openings or in areas where concentrated loads lead to tension stresses.

The basic idea for locally strengthened masonry walls consists of three principle steps: First, the description of the load-transfer within the structure; second, the behaviour between masonry and FRPs in the anchorage region; and third, the bond characteristics of single masonry units. *Ganz (1985)* already showed that the theory of stress fields can be used for masonry shear walls. This modelling technique can also be adapted for post strengthened masonry structures *Schwegler (1994)*. For the anchorage region it is important to consider the masonry texture. Masonry consists of bricks/blocks and mortar joints which can crack if FRP is under tension. Finally, the bond strength between a single masonry unit and FRP has to be known for different brick types, adhesives and FRPs.

## EXPERIMENTAL INVESTIGATIONS

### Material Characteristics

To investigate the bond characteristics of glass fibre-reinforced polymers (GFRP) and brick masonry, 33 single unit bond tests and six anchorage region tests on wall elements were carried out. In order to consider different strength performances, three different types of lime sand bricks and one type of clay brick were used. The strength characteristics are illustrated in Table 1. Moreover, two different adhesives were used to investigate effects of bond strength (Table 2). Values for tensile strength and density are given by the manufacturer.

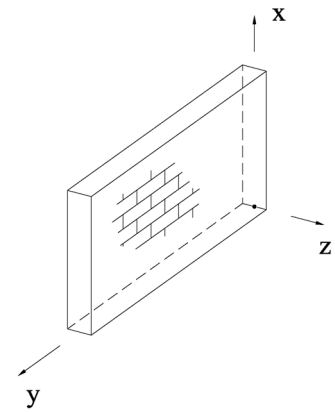


Figure 1. Coordinate system

Table 1. Types of masonry units and strength of single unit bond tests

	brick types	compression strength $f_{st,z}$ [N/mm <sup>2</sup> ]	surface tensile strength $f_{st,t,z}$ [N/mm <sup>2</sup> ]
KS12	solid lime-sand brick	22.61	1.70
KS20	solid lime-sand brick	22.76	2.24
KS28	solid lime-sand brick	29.82	1.81
Mz20	solid clay brick	35.17	2.17

Generally, compression tests were carried out using cylindrical specimens which were core-drilled perpendicular to bond surfaces. The surface tensile strengths were performed with a surface tension tester. For the determination of the surface tensile strength a circular steel stamp (diameter: 50 mm) was glued onto the brick surfaces and pulled off. The test procedure is documented in *Seim et al. (2008)*.

Table 2. Types and characteristics of adhesives

	adhesive	type	tensile strength [N/mm <sup>2</sup> ]	viscosity	density [kg/l]	colour
SD330	SikaDur 330	epoxy	30	high	1.31	grey
SP55	S&P Resin Epoxi 55	epoxy	35	low	1.11	transparent

For the anchorage tests two layer of glass fibre sheets were applied. One-layer was applied for unit bond tests. Laminate specimens were used to determine the sheet properties. Tension test procedure followed the German Code (*DIN EN 2747*). The characteristics of GFRPs are documented in Table 3.

Table 3. Characteristics of GFRP

	number of layers	tensile strength [kN/cm-width]	thickness [mm]	Young's modulus [N/mm <sup>2</sup> ]	part of fibre-volume of GFRP [%]
1L	1	1.93	0.64	20,159	22
2L	2	3.86	1.12	22,084	25

### Bond Tests - Single Masonry Unit

The test set-up consisted of a steel frame with hinges at top and bottom (Figures 2a). The bricks were placed into the frame on a steel plate at the bottom and the FRP sheet was anchored against a rounded steel block. The width of the FRP sheets was generally 70 mm. The predicted critical bond length was expected between 100 mm and 150 mm (eg. *Aiello et al. 2003*). Therefore the bond length was varied between 240 mm and 60 mm for lime-sand bricks KS20. The bricks were cleaned by compressed air before applying the first adhesive. FRP sheets were then pushed into the adhesive with a roller until adhesive seeped through the sheets. Finally, more adhesive was applied and distributed on top. All tests were loaded displacement controlled with a rate of 0.35 mm/minute.

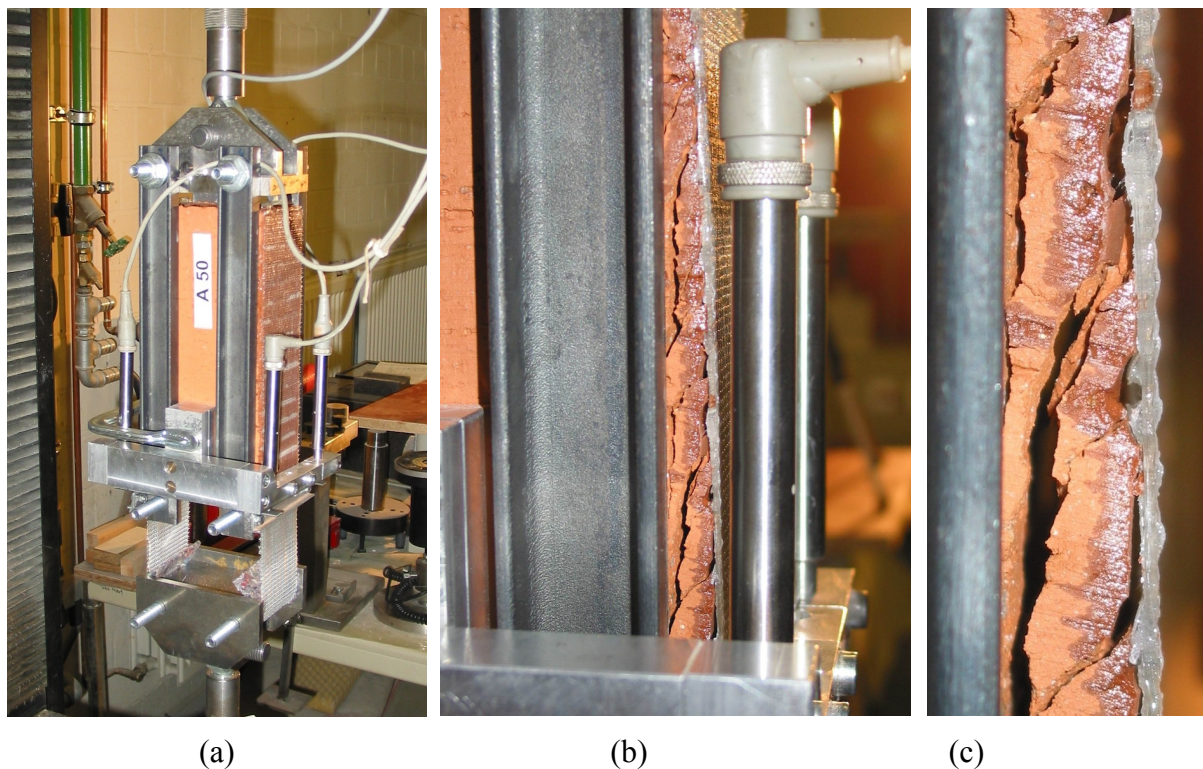


Figure 2. (a) test set-up of single masonry unit, (b) failure mode with tooth formation, (c) detail of “teeth” (Mz20-SP55-1L)

Generally, bond failure occurred in a brittle manner within the masonry units near the glued joint. The failure depth was influenced by the type of adhesive. Cohesion failure occurred in a

depth of approximately 2 mm (KS20) for SD330 adhesive and approximately 6 mm (Mz20) for SP55. Three stages with different bond characteristics were identified during the tests. The first one was a stage of intact bond between brick and FRP where no failure and no cracks were visible. The second was an intermediate stage between intact bond and bond failure. Here, teeth like shapes developed. The third stage was a complete bond failure (Figure 2b, c).

The “teeth” caused an increase of bond-strength depending on bond-length. Figure 3 illustrates two typical displacement-curves. Both graphs shows a nonlinear section and a nearly linear section. The transition of characteristics occurred then the first cracks were visible at the beginning of stage two. This point was defined as  $F_{u',exp}$ . Subsequent increase of bond-forces take place due to friction action. For masonry unit bond tests carried out with a bond length of 240 mm, friction action could be conservatively evaluated to five percent for lime sand bricks and twenty percent for clay bricks (Equation 1).

$$F_{u',exp} = \zeta \cdot F_{u,exp} \quad (1)$$

$\zeta = 0.95$  for lime-sand bricks

$\zeta = 0.80$  for clay brick (Mz20)

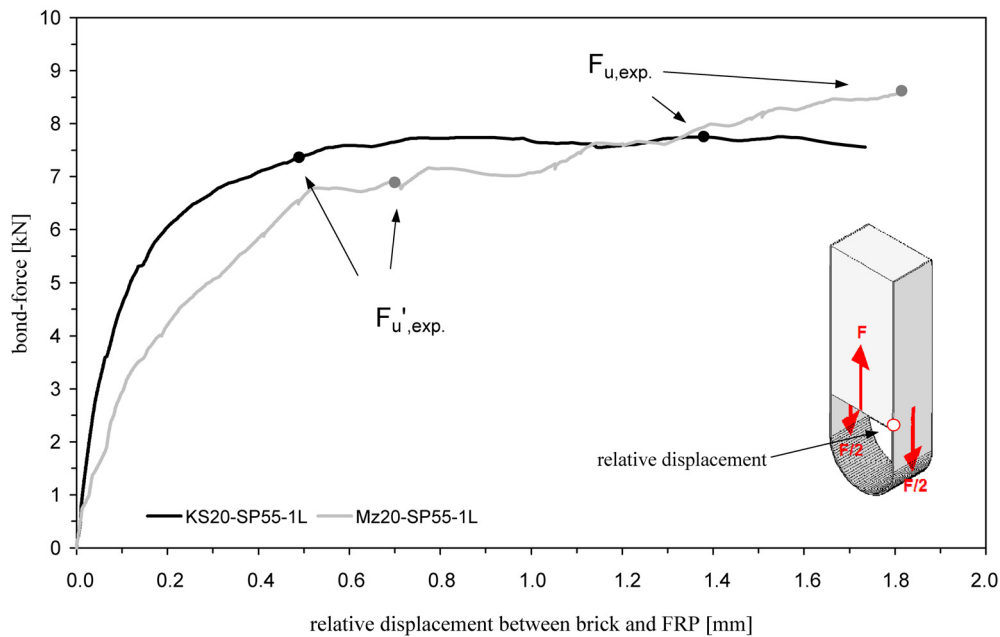


Figure 3. Typical load-displacement-curves for lime-sand bricks and clay brick

Failure loads of single masonry unit bond tests with a bond length of 240 mm are shown in Table 4. It should be noted, that the bond-forces are related to two bond planes, of one brick. It was observed, that bond-strength was dependent on the strength of bricks, where bond strength increased with increasing brick strength. In addition it was found that bond strength was also dependent on the type of adhesive. The results suggested that the adhesive with lower viscosity (*adhesive SP55*) achieved a higher strength.

Table 5 illustrates the results of tests with varied bond length. Comparison of the results with the results of Table 4 shows that the strength does not increase over a maximum bond load. This effect of a maximum bond-load with a corresponding critical bond-length was previously established for FRP strengthened concrete structures (e.g. *Schilde 2007*) and for masonry units and FRP (*Aiello et al. 2003*). The critical bond length was approximately 120 mm (KS20-SP55-L1).

Table 4. Results of bond tests with a bond-length of 240 mm

Test	$F_{u,exp.}$ [kN]	$F_{u',exp.}$ [kN]	$\bar{F}_{u',exp.}$ [kN]	Test	$F_{u,exp.}$ [kN]	$F_{u',exp.}$ [kN]	$\bar{F}_{u',exp.}$ [kN]
KS12-SD330-1L	9.90	9.41	9.10	KS12-SP55-1L	13.24	12.58	13.00
	9.16	8.70			14.12	13.41	
	9.68	9.20			13.68	13.00	
KS20-SD330-1L	9.54	9.06	9.46	KS20-SP55-1L	15.72	14.93	14.94
	10.58	10.05			15.96	15.16	
	9.76	9.27			15.50	14.73	
KS28-SD330-1L	14.10	13.40	13.40	KS28-SP55-1L	19.16	18.20	17.07
	14.14	13.43			17.92	17.02	
	14.06	13.36			16.82	15.98	
Mz20-SD330-1L	15.44	12.35	12.24	Mz20-SP55-1L	18.42	14.74	14.26
	16.00	12.80			17.38	13.90	
	14.46	11.57			17.24	13.79	

Table 5. Results of bond tests with a variation of bond-length

Test	bond-width [mm]	bond-length [mm]	$F_{u,exp.}$ [kN]	$\bar{F}_{u,exp.}$ [kN]
KS20-SP55-1L	70	180	17.07	16.12
	70	180	15.69	
	70	180	15.61	
KS20-SP55-1L	70	120	15.58	15.82
	70	120	15.72	
	70	120	16.16	
KS20-SP55-1L	70	60	14.32	13.96
	70	60	13.63	
	70	60	13.94	

### Anchorage Tests

The test set-up consisted of a 750 mm high, nearly 750 mm wide and 115 mm deep masonry wall element which represents an anchorage region (Figure 4a). For the first six out of 24 tests lime-sand bricks (KS20) were used in combination with a cement-lime mortar. Two layers of



FRP were glued perpendicular and parallel to the horizontal joints (Figure 4b, c) with SP55. This allowed the consideration of both principal load transfer directions of an in-plane loaded and locally post strengthened masonry wall. Compression stresses of  $0.60 \text{ N/mm}^2$  for AT1 to AT3 and  $0.15 \text{ N/mm}^2$  for AT4 to AT6 were used in the tests, to represent dead loads. The FRP was applied in a similar way as for the single masonry unit tests. Moreover the surfaces of the lime-sand brick wall elements were additionally cleaned with a steel brush. The tests were loaded displacement controlled with a rate of  $2 \text{ mm/minute}$ . The compressive strength of bricks was determined on cylindrical cores. Tensile strength was carried out as tensile surface strength by pull off of steel stamps (*Seim et al. 2008*). The compressive strength of mortar was determined with mortar-prisms (Table 6).

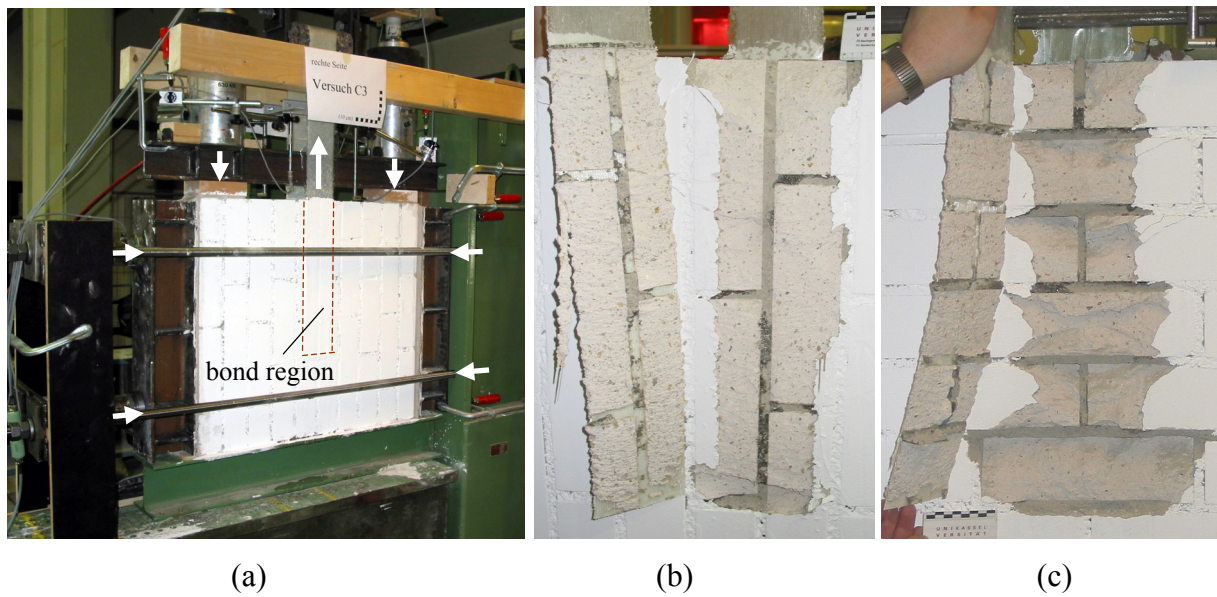


Figure 4. (a) set-up of anchorage tests, (b) bond failure for FRPs glued parallel to joints (test AT2) and (c) bond failure for FRPs glued perpendicular to joints (test AT4)

Three failure modes were observed (Table 7): friction failure of the horizontal masonry joints (AT1), rupture of FRP (AT5) and bond failure in terms of cohesion failure of bricks. In the case of bond failure, the decrease in resistance occurred step wise with sudden final failure. Cracks which were inclined diagonally from the bond region up to the bearings and the joints in this region opened up to  $2 \text{ mm}$ . Cohesion failure in the bricks occurred at a depth of approximately  $10 \text{ mm}$  to  $30 \text{ mm}$  (AT4).

Table 6. Specification of anchorage tests

Test	Test specification	$f_{st,x}$ [N/mm <sup>2</sup> ]	$f_{mo}$ [N/mm <sup>2</sup> ]	$f_{st,z}$ [N/mm <sup>2</sup> ]	$f_{st,t,z}$ [N/mm <sup>2</sup> ]
AT1	brick: KS20 adhesive: SP55	35.6	12.0	32.8	3.2
AT2			11.6		
AT3			13.0		
AT4		35.6	13.1	32.8	3.2
AT5			12.9		
AT6			11.7		

where:

- $f_{st,x}$  - compression strength of brick in masonry plane direction  
 $f_{mo}$  - compression strength of mortar (tested on prisms)  
 $f_{st,z}$  - compression strength of brick perpendicular to bond surface  
 $f_{st,t,z}$  - surface tensile strength perpendicular to bond surface

Ultimate bond forces for FRPs applied perpendicular to horizontal joints, were slightly higher than for parallel application. This is caused by a higher number of joints and in the consequence, a higher number of masonry units. It could be assumed, that a higher number of short masonry units lead to higher ultimate bond forces. For Tests AT4 to AT6 (Figure 4c) there were, in comparison to AT1 to AT3, outbreaks of a depth to 30 mm visible. For Test AT1 to AT3, the parallel gluing of FRP reduces this effect.

Table 7. Results of anchorage tests

Test	FRP direction	bond-width [mm]	bond-length [mm]	number of layers	$F_{u,exp.}$ [kN]	failure type
AT1	parallel to horizontal joints	100	490	2	75.9	friction failure of horizontal masonry joints
AT2					66.7	bond failure
AT3					66.3	friction failure of horizontal masonry joints
AT4	perpendicular to horizontal joints	100	490	2	73.8	bond failure
AT5					76.0	rupture of FRP
AT6					75.2	bond failure

## THEORETICAL INVESTIGATIONS

The theory of bond failure is based on a model of *Volkersen (1953)*, which was derived for the description of bond characteristics of riveted joints (Figure 5a-c). *Volkersen* described the bond characteristic with an additional layer that is dependent on implied bond-functions. These bond-functions are generally expressed as a shear stress-displacement-relation at the differential element. The bond forces on FRPs can be calculated with following equation:

$$F_f(l_b) = b_f \cdot \int_{x=0}^{x=l_b} \tau_b(x) dx \quad (2)$$

where:

$b_f, l_b$  - width and bond-length of FRP  
 $\tau_b(x)$  - shear stress at bond-length x

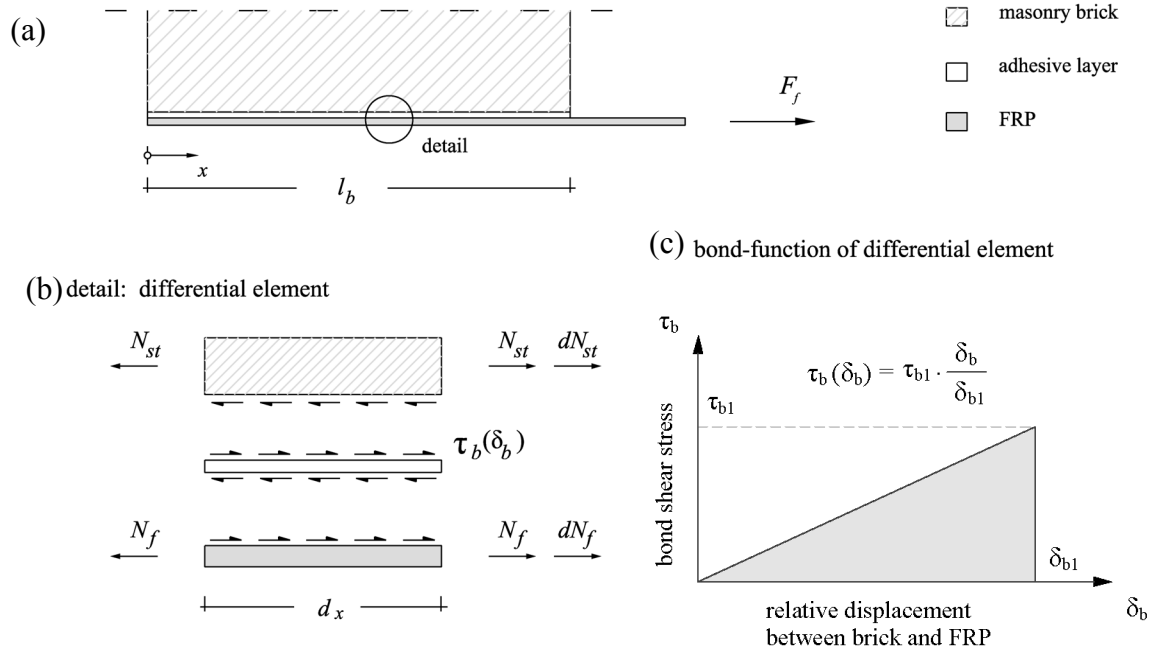


Figure 5. (a) bond geometry, (b) shear-forces at the differential element and (c) linear bond-function

Equation (2) can be solved for the differential bond-element with the following assumptions: The material characteristics are linear-elastic, there are no stresses perpendicular to the bond-joint and shear stress on the differential element are constant. This leads to the general solution:

$$\delta_b'' - \tau_b(\delta_b) \cdot \left( \frac{1}{E_f \cdot t_f} + \frac{1}{E_{st} \cdot t_{st}} \right) = 0 \quad (3)$$

and under consideration of the geometry and a linear bond-function (Figure 5c) to the bond-force  $F_f(l_b)$ :

$$F_f(l_b) = b_f \cdot \sqrt{2 \cdot G_b \cdot E_f \cdot t_f} \cdot \tanh(\omega \cdot l_b) \quad (4)$$

$$\omega = \sqrt{\frac{\tau_{b1}^2}{2 \cdot G_b \cdot E_f \cdot t_f}} \quad (5)$$

$$G_b = 0.5 \cdot \tau_{b1} \cdot \delta_{b1} \hat{=} c_b \cdot \sqrt{f_{st} \cdot f_{st,t}} \quad (6)$$

$$\tau_{b1} = 0.5 \cdot \sqrt{f_{st} \cdot f_{st,t}} \quad (7)$$



where:  $\delta_b$  - relative displacement in bond joint  
 $\tau_{b1}$  - maximum shear stress  
 $G_b$  - energy for complete bond failure  
 $c_b$  - adaptation factor  
 $f_{st}, f_{st,t}$  - compression and surface tensile strength perpendicular to glued surface

$G_b$  represents the energy for complete bond failure at the differential element and can be calculated as the integral of the considered bond-function. The energy is dependent on the maximum shear stress  $\tau_{b1}$  which can be calculated with the *Mohr-Coulomb-Criterion* and the relative displacement  $\delta_{b1}$ , where the latter is very difficult to measure. Alternatively, the energy  $G_b$  can be described using the compression and tensile strength, generally the surface tensile strength, of the bricks and an adaptation factor  $c_b$  (Equation 6). This factor is dependent on the types of adhesives and was evaluated as 0.035 for SD330 and 0.06 for SP55. The comparison of the experimental and analytical results offered a good correspondence (Figure 6). This reinforces the idea that ultimate bond-forces are, beside the FRP characteristics and bond geometries, mainly dependent on the strength of bricks and adhesive.

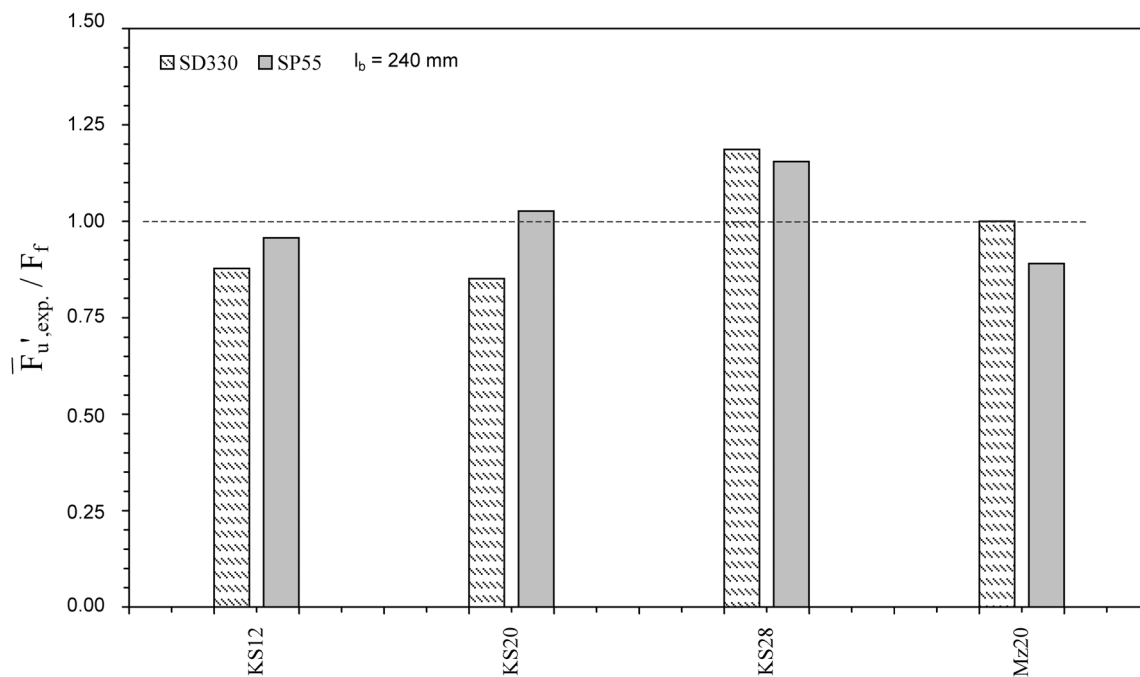


Figure 6. Comparison of experimental and analytical ultimate bond-forces of masonry units

## CONCLUSIONS

33 bond tests on single masonry units and six anchorage tests on wall elements were carried out. Three types of lime-sand bricks and one type of clay brick were tested in combination with two types of epoxy adhesives and one type of glass fibre sheet. In addition the bond-length was varied. Generally, the failure mode occurred in a brittle manner as a cohesion failure near the glued surfaces within the bricks. It was clearly found that ultimate bond-

forces depend on strength characteristics of bricks and adhesives. An adhesive with lower viscosity and bricks with higher strengths lead to higher bond-strengths. A maximum bond-load connected to a maximum bond-length could be detected. The proposed bond model enables the calculation of bond-forces in relation to bond-lengths. The ultimate bond-force can be calculated with  $\tanh(\omega \cdot l_b)$  (Equation 4). For calculation of bond-forces, it should be used both: the compression and tensile strength. The maximum of differences between experimental and analytical results was 18 %. For anchorage tests three types of failure were observed: rupture of FRP, friction failure in the horizontal masonry joints and bond failure in terms of cohesion failure within the bricks. In the cases of bond failure, the decrease in resistance occurred step wise with sudden final failure. Cracks which were inclined diagonally from the bond region up to the bearings and the joints in this region opened up to 2 mm. Cohesion failure in the bricks occurred in a depth of approximately 10 mm to 30 mm.

More investigations with different types of single masonry units in connection with GFRP and CFRP, anchorage tests with the variation of the bond-length and bond-width of FRP and locally strengthened full-scale tests will be presented in future publications.

## REFERENCES

- Aiello, M. A.; Scolti, M. S., "Bond analysis of masonry structures strengthened with CFRP sheets", *Construction and Building Materials*, Vol. 20, 90-100, 2006.
- DIN EN 2747, "Glasfaserverstärkte Kunststoffe: Zugversuch", *Beuth Verlag Berlin*, Oktober, 1998.
- ElGawady, M., "Seismic In-Plane behavior of URM Walls Upgraded with Composites", Phd-Thesis, *EPFL Lausanne*, 2004.
- Ganz, H. R., "Mauerwerksscheiben unter Normalkraft und Schub", Report Nr. 148, Institut für Baustatik und Konstruktion ETH Zürich, *Brinkhäuser Verlag*, 1985.
- Schilde K., Seim W., "Experimental and numerical investigations of bond between CFRP and concrete", *Construction and Building Materials*, Vol. 21, No. 4, 2007.
- Schwegler, G., "Verstärken von Mauerwerk mit Faserverbundwerkstoffen in seismisch gefährdeten Zonen", Technical Report, *Eidgenössische Materialprüfungs- und Forschungsanstalt (EMPA)*, Dübendorf, Swiss, 1994.
- Seim, W.; Humburg, E.; Stürz, J., "Local post-strengthening of masonry walls by use of fiber-reinforced polymers (FRP)", *Composites in Construction*, University of Calabria, Rende, 2003.
- Seim, W.; Pfeiffer, U.; Hempel, M.; Orschulok, R., "A new method to investigate the surface tensile strength of concrete and masonry structures", *Proceedings of 14<sup>th</sup> International Brick and Block Conference*, Sydney, 17-20 February, 2008.
- Wallner, C.; Stempniewski, L., "Experiments on seismic retrofitting of in-plane loaded masonry walls with fibre composites", *WIT Transactions on the Built Environment*, Vol. 81, 2005.
- Volkersen, O., "Die Schubkraftverteilung in Leim-, Niet- und Bolzenverbindungen", *Energie und Technik*, Heft 3/ 5/ 7, March, 1953.